

Path-length distributions, scattering, and absorption in refractive spheres and slabsMatt Majic^{✉,*}, Walter R. C. Somerville^{✉,†} and Eric C. Le Ru[‡]*The MacDiarmid Institute for Advanced Materials and Nanotechnology School of Chemical and Physical Sciences Victoria, University of Wellington, PO Box 600, Wellington, New Zealand*

(Received 11 November 2022; accepted 10 April 2023; published 12 May 2023)

We derive the path-length distribution (PLD) of light rays diffusely incident on a refractive sphere and slab in the geometric optics case. Refraction affects the width of the distribution and internal reflection introduces longer path lengths. Polarization is also taken into account and has a minor effect on the shape. For the slab, we also consider the effect of a small amount of scattering in the medium which adds to the tail of the PLD and significantly increases the mean path length. The absorption is calculated from the PLD, from which we approximate the absorption in the slab and sphere to the second order in the absorption coefficient, and also to the second order in the scattering coefficient for the slab.

DOI: [10.1103/PhysRevA.107.053509](https://doi.org/10.1103/PhysRevA.107.053509)**I. INTRODUCTION**

In geometric optics, the path length of a light ray through some object is important for understanding quantities such as absorption. An object's absorption is calculated in the geometrical optics limit as the integral over the path-length distribution (PLD) of light rays, weighted by an exponential absorption factor. Alternatively, the mean path length provides a simple approximation to the absorption in the weakly absorbing limit. There has been recent progress on the mean path length in refractive objects [1–5]—in particular, the mean path length theorem provides a general formula in the case of scattering [1,2]. However, to move beyond the weakly absorbing approximation, we need to study PLDs. Chord-length distributions with no refraction effects have been studied analytically for objects such as triangles, spheres, and prisms [6], but PLDs accounting for reflection, refraction, and polarization are much more complex. For example, the scattering properties of atmospheric aerosol particles are currently modeled with PLDs obtained from numerical ray tracing [7]. Analytically, chord-length distributions (not accounting for reflection and refraction) have been derived for the sphere and cube, but refractive effects are still modeled empirically [8], or ignored [9]. The PLDs of light in an infinite slab are crucial to study absorption of photovoltaic cells [10] and of refracting ice layers [11], and they have been studied numerically and analytically in the low scattering limit for a slab under normal incidence [12]. It is well known that adding a scattering mechanism, e.g., a rough boundary or diffusing medium, enhances the absorption of light in a dielectric slab, and this is used to increase the efficiency of solar cells.

In this paper we derive exact analytic expressions for the PLD in a refracting infinite slab and a sphere, for dif-

fusely incident light from all directions. While the sphere and slab geometry have exact electromagnetic solutions for their absorption properties, this is not true for more complex geometries where geometric optics is a more necessary approach. This study aims to provide the first step toward obtaining analytic results for PLDs in more complex geometries. These are validated against numerical Monte Carlo ray tracing simulations. We consider the effect of a scattering coefficient and derive an approximate PLD in the weak scattering limit for the slab. We then use these distributions to calculate the absorption and expand it to second order in both scattering and absorption coefficients.

II. PATH-LENGTH DISTRIBUTION

In this section we derive analytical expressions for the PLD in spheres and infinite slabs.

A. Reflection and refraction at an interface

In general we consider an external medium 1 with refractive index n_1 , encompassing a medium 2 with refractive index $n_2 > n_1$, of which we are measuring the path lengths of the rays inside. We assume that the dielectric constants are both real, and that the wavelength of the light is sufficiently small compared to the geometry that the geometric optics approximation can be applied. A ray from medium 1 enters medium 2 with an angle θ_1 to the normal. With some probability (presented below), the ray may either reflect back into medium 1 with angle θ_1 , or refract into medium 2 with angle θ_2 determined by Snell's law,

$$\sin \theta_2 = \frac{\sin \theta_1}{s}, \quad (1)$$

where $s = n_2/n_1$. θ_2 will never exceed the critical angle $\theta_c = \text{asin}(1/s)$ (within geometric optics), and any ray traveling from medium 2 to medium 1 cannot refract through the boundary if $\theta_2 > \theta_c$: in this case, it will undergo total internal

*mattmajic@gmail.com

†walter.somerville@vuw.ac.nz

‡Eric.LeRu@vuw.ac.nz

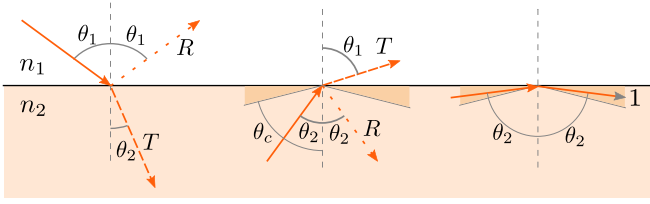


FIG. 1. Refraction and reflection at an interface for a ray (red arrows) heading from medium 1 to 2 (left) or vice versa (middle, right). T and R are the probabilities of transmission and reflection. The sparsely dotted lines indicate a low probability of occurrence (typically $T \gg R$), and the darker shading indicates angles above θ_c for which total internal reflection occurs if $\theta_2 > \theta_c$.

reflection with a probability of 1. The possible scenarios are illustrated in Fig. 1.

Unlike when simply calculating the mean path length, we must also consider polarization. For purposes of calculating PLDs, any ray that hits the surface can be split into components of s and p polarization (electric field or magnetic field parallel to the surface),¹ and the probability of refracting through the boundary is given by the Fresnel transmission coefficients T_s and T_p [13]:

$$\begin{aligned} T_s &= \frac{4s \cos \theta_1 \cos \theta_2}{(\cos \theta_1 + s \cos \theta_2)^2} \\ T_p &= \frac{4s \cos \theta_1 \cos \theta_2}{(\cos \theta_2 + s \cos \theta_1)^2}, \end{aligned} \quad (2)$$

where θ_1, θ_2 are related through (1). These give both the probability that a ray will refract from medium 1 to 2, or from medium 2 to 1. The probabilities of reflectance are then $R_p = 1 - T_p$ and $R_s = 1 - T_s$.

B. Sphere

Consider a sphere of radius a and a ray that is refracted inward at an angle θ_2 (see inset of Fig. 2). The chord length C of this ray is

$$C = 2a \cos \theta_2. \quad (3)$$

Note that the path length L is the total path of the ray inside medium 2, which may include multiple chords. We start with an expression for the mean chord length, which is obtained from an integral over all possible angles of incidence $0 \leq \theta_1 < \pi/2$, or equivalently over $0 \leq \theta_2 < \theta_c$. It was noted in Ref. [2] that all probabilistic reflections (not including total internal reflection) could be ignored and replaced by refractions when calculating the mean path length. This means that in objects where total internal reflections are inaccessible from

¹This is physically not the same as a ray with mixed polarization, but in the limit of infinitely many rays the probability outcomes of reflection and refraction are the same. To be safe, in our Monte Carlo codes we did not assume that rays could split into s and p components and gave each ray a random polarization vector (mixed s and p).

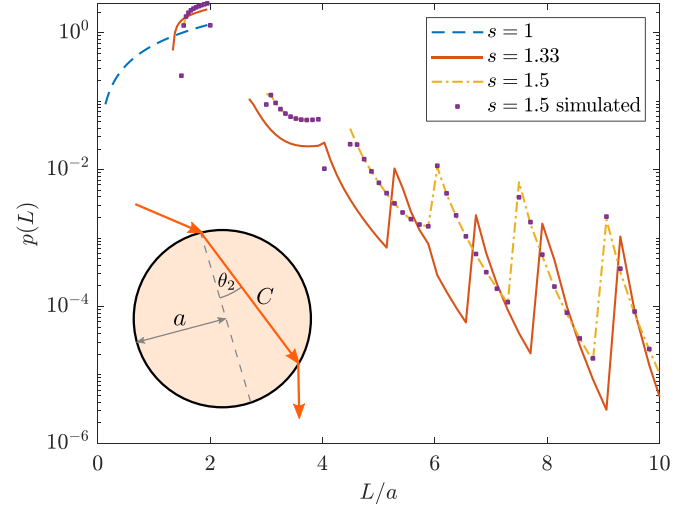


FIG. 2. Path-length distribution Eq. (11) $p(L)$ for path length L in a sphere of radius a . Numerical results are compared for $s = 1.5$ (numerical results compare well for $s = 1, 1.33$ also). $s = 1$ is the chord-length distribution through an imaginary sphere boundary. Inset: diagram of an example chord of length C in a sphere, where in this case $L = C$ since there are no internal reflections.

outside (like the sphere), the mean path length $\langle L \rangle$ and mean chord length $\langle C \rangle$ are equal:

$$\langle L_{\text{sph}} \rangle = \langle C_{\text{sph}} \rangle = 2s^2 \int_0^{\theta_c} C(\theta_2) \cos \theta_2 \sin \theta_2 d\theta_2 \quad (4)$$

$$= \frac{4a}{3} s^2 \left[1 - \left(1 - \frac{1}{s^2} \right)^{3/2} \right]. \quad (5)$$

The integral (4) encodes the chord-length distribution $p_{\text{chd}}(c)$, which can be extracted by expressing the mean chord length as an integral over C :

$$\langle C_{\text{sph}} \rangle = \int_0^\infty p_{\text{chd}}(C) C dC. \quad (6)$$

Comparing the integrals (4) and (6) through the relationship (3) reveals the chord-length distribution:

$$p_{\text{chd}}(C) = \frac{s^2 C}{2a^2} \Theta(2a \cos \theta_c \leq C \leq 2a) \quad (7)$$

where $\Theta(\text{condition}) = 1$ if the condition is met and 0 otherwise.

To find the PLD, we need to account for probabilistic reflections inside the sphere, using the Fresnel coefficients. For the sphere and slab, the polarization of rays relative to the surface is the same at each reflection, so we can treat p and s polarizations separately.

We will break down the PLD into a sum over contributions from rays with n chords, starting with $n = 1$ for rays that enter and do not internally reflect, with distribution $p_1(L)$. The fraction of these rays compared to the total number incident on the sphere is equal to the probability of entering the sphere, T_j (for $j = p$ or s), times the probability of leaving the sphere T_j on the second contact with the surface. By using Snell's law (1) and inverting the relationship (3), we can express the transmittance in terms of chord length, writing $T_j(C)$,

$R_j(C)$. These rays are distributed according to the distribution $p_1(L) = p_{\text{chd}}(C)$ (note that $L = C$ for the case of p_1). p_{chd} is normalized to have a total probability of 1, so in the expression for the total PLD we will multiply p_1 by the probability $T_j(C)^2$ of a ray having a single chord.

The probability of a ray having n chords is equal to the probability that the ray enters, reflects $n - 1$ times inside, and then leaves, which is $R_j(C)^{n-1}T_j(C)^2$. The PLD of these rays is

$$p_n(L) = \frac{1}{n} p_{\text{chd}}\left(\frac{L}{n}\right), \quad (8)$$

where $L/n = C$ is the chord length and the $1/n$ factor normalizes $p_n(L)$.

Note that standard expressions for mean path length include the average incident rays that reflect directly off the object (rays of zero path length). For completeness, we also include these rays in our distributions. These are described by the delta function $\delta(L)$. Of the total, these make up a fraction R_F , the average of the reflection coefficients over all angles [14]:

$$\begin{aligned} R_F &= \int_0^{\pi/2} 2 \cos \theta \sin \theta [R_{12}^s(\theta) + R_{12}^p(\theta)] d\theta \\ &= \frac{1}{2} + \frac{(s-1)(3s+1)}{6(s+1)^2} - \frac{2s^3(s^2+2s-1)}{(s^4-1)(s^2+1)} \\ &\quad + \frac{8s^4(s^4+1) \ln s}{(s^4-1)^2(s^2+1)} + \frac{s^2(s^2-1)^2}{(s^2+1)^3} \ln \frac{s-1}{s+1}. \end{aligned} \quad (9)$$

The complete PLD is then the sum over the PLD for n chords, and over the polarizations $j = s, p$:

$$p(L) = R_F \delta(L) + \frac{1}{2} \sum_{j=s,p} \sum_{n=1}^{\infty} R_j(C)^{n-1} T_j(C)^2 p_n(L), \quad (10)$$

which can be expressed more explicitly using (8) and (7):

$$\begin{aligned} p(L) &= R_F \delta(L) + \sum_{j=s,p} \sum_{n=1}^{\infty} \frac{s^2 L}{4a^2 n^2} R_j\left(\frac{L}{n}\right)^{n-1} T_j\left(\frac{L}{n}\right)^2 \\ &\quad \Theta\left(2a \cos \theta_c \leq \frac{L}{n} \leq 2a\right). \end{aligned} \quad (11)$$

Again, note that for each n , $C = L/n$ is the chord length. This distribution is plotted in Fig. 2, and agrees with Monte Carlo simulations of 10^8 rays to an accuracy of 10^{-3} – 10^{-2} for $L/a < 5$ (the simulation accuracy decreases with L since fewer rays have long L). Figure 2 corrects Fig. 6(b) of Ref. [9], which did not account for effects of transmission probability, probabilistic reflection, or polarization. The discontinuities (including the gap at $L \gtrsim 2a$) in the PLDs shown in Fig. 2 arise from the minimum and maximum chord lengths in the Heaviside theta function in (11).

Note that while this expression is technically an infinite series, each term only contributes to a confined range of L , so it can be truncated at a finite n with zero loss of precision below a certain range of L . If one is interested in a range of, say, $0 < L < 10a$, then only about ten terms are needed for full precision (depending on s).

We can check analytically that the sum of all probabilities is normalized:

$$\begin{aligned} &\int_0^{\infty} p(L) dL \\ &= R_F + \frac{1}{2} \sum_{j=s,p} \sum_{n=1}^{\infty} \int_{2a \cos \theta_c}^{2an} R_j\left(\frac{L}{n}\right)^{n-1} T_j\left(\frac{L}{n}\right)^2 p_n(L) dL \\ &= R_F + \frac{1}{2} \sum_{j=s,p} \sum_{n=1}^{\infty} \int_{2a \cos \theta_c}^{2a} R_j(C)^{n-1} T_j(C)^2 \frac{p_{\text{chd}}(C)}{n} n dC \\ &= R_F + \frac{1}{2} \sum_{j=s,p} \int_{2a \cos \theta_c}^{2a} T_j(C) p_{\text{chd}}(C) dC \\ &= R_F + \frac{s^2}{2} \sum_{j=s,p} \int_0^{\theta_c} T_{21}^j(\theta_2) 2 \cos \theta_2 \sin \theta_2 d\theta_2 = 1. \end{aligned} \quad (12)$$

The third equality above uses the geometric series $\sum_{n=1}^{\infty} R_j^{n-1} = 1/T_j$, and the last integral is the average transmittance from medium 2 to medium 1, which is simply $T_F = 1 - R_F$.

Similarly, one can check that the mean path length of this distribution $\langle L \rangle = \int_0^{\infty} L p(L) dL$ evaluates to (5).

C. Infinite slab

Like the sphere, each point on the surface of an infinite slab (e.g., defined as occupying $0 \leq z \leq a$) is equivalent by symmetry. The relationship between the chord length C and angle θ_2 is

$$C = \frac{a}{\cos \theta_2} \quad (13)$$

and the chord-length distribution is

$$p_{\text{chd}}(C) = \frac{2s^2 a^2}{C^3} \Theta\left(a \leq C \leq \frac{a}{\cos \theta_c}\right). \quad (14)$$

Again, when a ray reflects, it has the same angle and chord length, so a ray that reflects n times has path length $L = nC$. The PLD is then

$$\begin{aligned} p(L) &= R_F \delta(L) + \sum_{j=s,p} \sum_{n=1}^{\infty} \frac{s^2 a^2 n^2}{L^3} R_j\left(\frac{L}{n}\right)^{n-1} T_j\left(\frac{L}{n}\right)^2 \\ &\quad \Theta\left(a \leq \frac{L}{n} \leq \frac{a}{\cos \theta_c}\right), \end{aligned} \quad (15)$$

which is plotted in Fig. 3, and has been checked to match Monte-Carlo simulations of 10^8 rays to within a relative error of $10^{-3} \sim 10^{-2}$.

III. WEAK SCATTERING

For refractive objects, weak scattering is not just a second-order effect. Recall that the mean path length differs in the case of zero scattering versus with scattering, which is independent of the scattering coefficient. There is a discontinuity at zero scattering, and this was somewhat addressed in Ref. [2], but without explicit calculation of PLDs, which we set out to do here. Specifically, we want to show that when

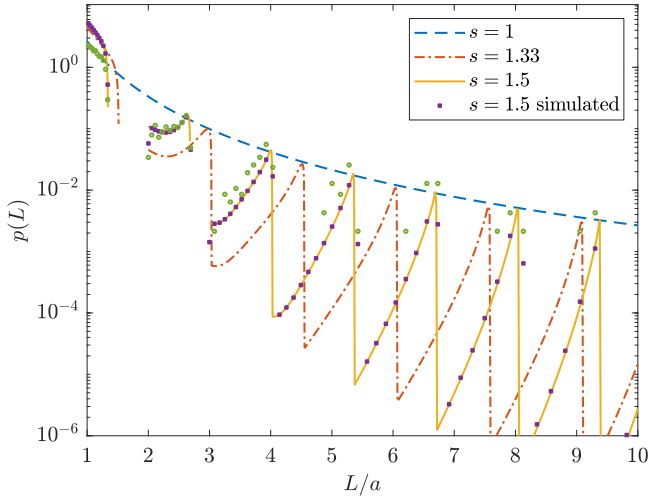


FIG. 3. Path-length distribution Eq. (15) for a slab of thickness a . Numerical results for 10^9 rays are compared for $s = 1.5$ (numerical results compare well for $s = 1, 1.33$ also).

an arbitrarily small scattering coefficient is added, we can approximate the effect of this on the PLD, and find that the mean path length is equal to that in the scattering case.

For weak scattering, the main effect on the PLD is the presence of trapped modes which indefinitely undergo total internal reflection until they scatter again. A ray cannot enter a trapped mode if it refracts into the object from medium 1, but scattering allows a ray to enter such a mode.

To model minor imperfections in the material, we give rays a small probability α_s per unit length of scattering to an isotropically random direction. We will focus on the slab because in a sphere the density of rays is not uniform [4], which complicates derivations.

The probability of a ray scattering at all is $\alpha_s \langle L \rangle$, and we consider the limit $\alpha_s \langle L \rangle \rightarrow 0$. When a ray scatters it lands in either a free mode with some probability P_F , which is a trajectory that could be populated via refraction from outside, or a trapped mode with probability $P_T = 1 - P_F$, which is inaccessible from outside and can only be occupied via scattering. In a slab, P_T is calculated as the range of angles available via isotropic scattering that correspond to total internal reflection. The isotropic probability distribution for scattering to an angle θ is $p_\theta(\theta) = \sin \theta$, and $P_T = \int_{\theta_c}^{\pi/2} p_\theta(\theta) d\theta = \cos \theta_c$ (in a sphere we cannot use such a simple calculation as rays have a different probability of trapping depending on their position).

One can divide the PLD into contributions from rays that do not scatter, $p_0(L)$ [given in Eqs. (11) and (15)], rays that scatter but do not become trapped, $p_S(L)$, and those that become trapped, $p_T(L)$. The total PLD is then

$$p(L) = (1 - \alpha_s \langle L \rangle) p_0(L) + \alpha_s \langle L \rangle [P_F p_S(L) + P_T p_T(L)]. \quad (16)$$

We will now make some observations and justify some approximations towards obtaining a simplified expression for the PLD in the low-scattering case.

(1) If the scattering coefficient α_s is small, rays that scatter into trapped modes, with PLD $p_T(L)$, will not escape for a long time and therefore have a very long path length. These

are the rays we are interested in because they have a significant impact on the PLD for large L .

(2) Rays that scatter into free modes, with PLD $p_S(L)$, are both rare and have short path lengths. While short path lengths may be interesting in some cases, we are ultimately interested in absorption, for which these rays will have minimal effect. We will ignore them altogether and set $p_S(L) = 0$.

(3) Scattered rays may scatter from one trapped mode to another. This is something we must account for, since the probability of landing in a trapped mode after scattering is significant, and the increase in path length is also significant.

(4) Trapped rays may scatter out of a trapped mode and then scatter back in to a different trapped mode, but the odds of this are small since it has to scatter twice before leaving. The fraction of rays that do this is of the order of $(\alpha_s \langle L \rangle)^2$, so we may ignore contributions from these rays. This approximation will slightly underestimate the length of trapped rays.

(5) Trapped rays occur via scattering through a free mode, and then leave the medium by scattering into a free mode. The distance traveled in these free modes is likely much less than the distance traveled in trapped modes, so for simplicity we may ignore the contributions at the beginning and end of the path. This approximation will again slightly underestimate the path lengths of trapped rays.

With simplifications 4 and 5, the trapped rays effectively undergo a simple random process where they have a constant probability per unit length $\alpha_s P_F$ of escaping instantly. This has the PLD of an exponential:

$$p_T(L) = \alpha_s P_F e^{-\alpha_s P_F L}, \quad (17)$$

which with Eq. (16) [and setting $p_S(L) = 0$] provides the PLD of rays incident on a slab with a small scattering probability throughout the medium.

One can check that Eq. (16) has a mean path length of $2as^2$ to zeroth order in $\alpha_s \langle L \rangle$, which is the invariant mean path length in a slab with scattering [1,2,15]. Equation (16) is plotted in Fig. 4 against Monte Carlo simulation data with 10^7 rays for a slab with $s = 1.5$, $a = 1$, and $\alpha_s = 0.0375$.

The absence of $p_S(L)$ is apparent in Fig. 4 for short path lengths. $p_S(L)$ is complicated to derive; we found rough approximations by ignoring reflections, but even these have complex piecewise expressions, so we decided not to present them. More importantly, the distribution for large L is fitted well by $p_T(L)$ of (17). These longer path lengths have a significant effect on absorption.

IV. ABSORPTION

We compute the absorption as the fraction of rays that are absorbed compared to the total number that hit the sample, including rays that are reflected straight off the surface. A simple model for an absorbing medium is where rays are absorbed with a probability per unit time, governed by an absorption coefficient α_a such that they travel a mean distance of $1/\alpha_a$ before absorption (assuming they do not leave the medium).

An object's absorption is an integral over the PLD:

$$A = 1 - \int_0^\infty e^{-\alpha_a L} p(L) dL. \quad (18)$$

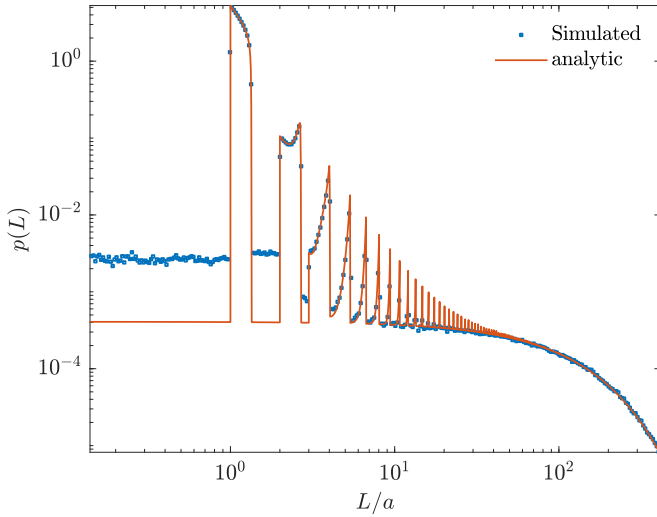


FIG. 4. Path-length distribution (16), with $p_S(L) = 0$ and $P_{TV}(L)$ from (17), compared to numerical simulations in a slab with $s = 1.5$, $a = 1$, and a low scattering coefficient $\alpha = 0.0375$.

Note that this equation uses the PLD from Eq. (11) or (15), even though the distribution itself is then modified by the absorption.

For the sphere and the slab, ignoring scattering, we can substitute the PLD (11) or (15) into the absorption integral (18). Using Eq. (10),

$$A = T_F - \frac{1}{2} \sum_{j=s,p} \sum_{n=1}^{\infty} \int_0^{\infty} R_j^{n-1}(C) T_j^2(C) p_n(nC) e^{-\alpha n C} dC, \quad (19)$$

where the integral bounds are confined by the Θ constraints in $p_{\text{chd}}(C)$. Following the simplifications in Eq. (12), using the closed form of the series over n , we can simplify this to

$$A = T_F - \frac{1}{2} \sum_{j=s,p} \int_0^{\infty} \frac{T_j(C)^2 p_{\text{chd}}(C)}{e^{\alpha a L} - R_j(C)} dC, \quad (20)$$

For the sphere, this expression is equivalent (with some manipulation) to the integral for the absorption efficiency for plane wave incidence, presented in Refs. [16,17]. It is also in Ref. [18] [Eq. (7.1)] but with the error that the absorption of different polarizations is not added separately.

In the low absorption limit, $\alpha_a \rightarrow 0$, the integrand in (18) may be expanded in a Taylor series, giving

$$A = \alpha_a \langle L \rangle - \frac{\alpha_a^2 a^2}{2} A^{(2)} + O(\alpha_a^3 a^3). \quad (21)$$

The first term is the standard approximation that the absorption is proportional to the mean path length in the weak absorbing limit. The second-order correction $A^{(2)}$ can be evaluated analytically from (19), using the series $\sum_{n=1}^{\infty} n^2 R^{n-1} = \frac{1+R}{(1-R)^3}$ and integrating. For the sphere,

$$A_{\text{sph}}^{(2)} = (s^2 + 1) \frac{s(s^2 + 6s^2 - 3) - (s^2 - 3)(s^2 - 1)^2 \coth^{-1}(s)}{4s^2}, \quad (22)$$

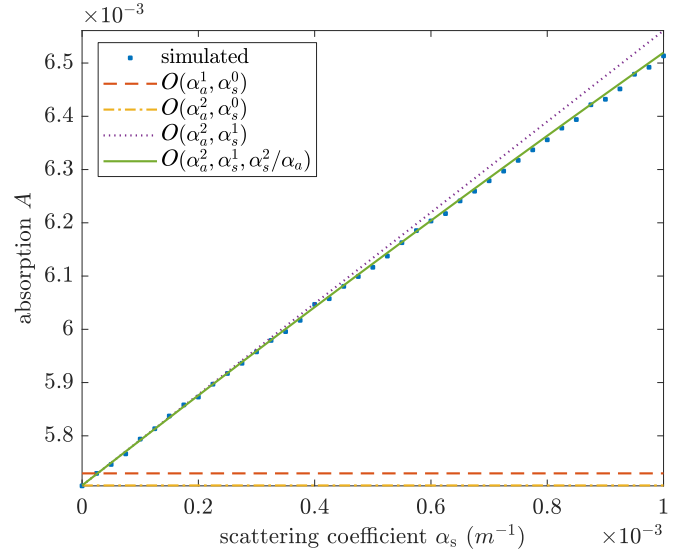


FIG. 5. Approximations for the absorption in a slab with $a = 1$, $s = 1.5$, a low absorption coefficient $\alpha_a = 0.005$, and a lower scattering coefficient α_s on the horizontal axis. The approximations in the legend correspond to including each term in (27) from left to right, e.g., the $O(\alpha_a^2, \alpha_s^1)$ line includes the first three terms.

and for the slab,

$$A_{\text{slb}}^{(2)} = -\frac{s^2 + 1}{2} [(s^2 + 1) \coth^{-1}(s) - s]. \quad (23)$$

One problem with $A_{\text{slb}}^{(2)}$ is that it diverges for $s \rightarrow 1$, because the maximum chord lengths approach infinity—the series (18) breaks down at order α_s^2 . This may be related to the fact that infinitely long chords exist for $s = 1$. The approximation $A_{\text{slb}}^{(2)}$ is still good for larger values of s —see Fig. 5 for $s = 1.5$. For $s = 1$, the absorption can be expanded as a series with a logarithmic term in α :

$$A_{\text{slb}}(s=1) = 2\alpha_a a + \left[\log(\alpha_a a) + \gamma - \frac{3}{2} \right] \alpha_a^2 a^2 + O(\alpha_a^3 a^3), \quad (24)$$

where $\gamma = 0.5772\dots$ is the Euler-Mascheroni constant. Note that the case $s = 1$ is just the absorption through a region of space with no refractive boundary.

We may now consider scattering. The approximation (21) requires that there are no significant contributions from $p(L)$ for large L comparable to $1/\alpha_a$, which may not be true when there is a significant scattering coefficient α_s . As discussed in Ref. [2], it still holds in the limit of low absorption but lower scattering.² We want to amend the approximation (21) to

²A similar formula to (21) appears in Ref. [19] [first-order term in their Eq. (1)] but where the mean path length $\langle L \rangle$ is taken to be the value when scattering occurs, $\langle L_{\text{sca}} \rangle$. However, that formula only holds for significantly lower absorption than scattering $\alpha_a \ll \alpha_s$, so that the absorption mean path length does not affect the long-lived scattered rays in trapped modes. Our numerical simulations confirm this, but the focus of this paper is on the limit of low scattering.

include higher-order terms in α_s , in the limit $\alpha_s \ll \alpha_a \ll 1/L$. This can only be done for the slab, using the results of Sec. III.

We plug the PLD with scattering (16) into the integral (18):

$$A_{\text{slb}} = 1 - \int_0^\infty e^{-\alpha_a L} [(1 - \alpha_s P_T \langle L \rangle) p_0(L) + \alpha_s P_T \langle L \rangle p_T(L)] dL. \quad (25)$$

We can evaluate the integral over $p_0(L)$ to second order in α_a using (21), while $p_T(L)$ is given in (17) as an exponential whose integral can be evaluated exactly:

$$\begin{aligned} \int_0^\infty e^{-\alpha_a L} p_T(L) dL &= \int_0^\infty \alpha_s P_F e^{-(\alpha_a + \alpha_s P_F) L} dL \\ &= \frac{\alpha_s^2 P_F}{\alpha_a + \alpha_s P_F}. \end{aligned} \quad (26)$$

So the total absorption is, discounting terms of order $\alpha_a \alpha_s \langle L \rangle^2$ or higher,

$$A_{\text{slb}} \approx \alpha_a \langle L \rangle - \frac{\alpha_a^2 a^2}{2} A_{\text{slb}}^{(2)} + \alpha_s P_T \langle L \rangle - \frac{\alpha_s^2 P_F P_T \langle L \rangle}{\alpha_a + \alpha_s P_F}. \quad (27)$$

This is plotted in Fig. 5 for small absorption and decreasing scattering, and shows excellent agreement with numerical simulations. The addition of each of the terms improves the approximation significantly. The first two terms of order $\alpha_a \langle L \rangle$ and $(\alpha_a \langle L \rangle)^2$ approximate the absorption for the case of no scattering. The third term of order α_s accounts for the absorption of trapped rays assuming that all trapped rays are absorbed. The last term is of order $\alpha_s^2 / \alpha_a \langle L \rangle$, which corrects the third term by accounting for the small probability that trapped rays may escape before being absorbed.

V. DISCUSSION AND CONCLUSION

We have derived PLDs for rays diffusely incident on a refracting sphere and a slab. For the slab we were also able to add scattering and approximate the PLDs in the low-scattering limit. We then used these PLDs to calculate the absorption, and found simple approximations for the absorption for low absorption and lower scattering, which matched Monte Carlo simulations accurately. These could, for example, provide simple approximations for absorption in atmospheric aerosols such as ice crystals or microplastics and for solar luminescent concentrators. The analytic results for PLDs were obtainable for a sphere and slab due to their high symmetry. In these geometries the chord length of each ray depends on angle only, and does not change from reflection to reflection, rays do not undergo total internal reflection, and the polarization relative to the surface does not change between reflections. The infinite cylinder satisfies these properties, except that polarization changes between reflections, so s and p components cannot be added separately. We treat the cylinder in the Appendix, but with making the nonphysical simplification of ignoring polarization. Still, the results are shown to compare reasonably well with numerical simulations, because polarization only affects the distributions slightly. Nonpolarized PLDs are still potentially interest-

ing as they may apply to high-frequency pressure or sound waves.

ACKNOWLEDGMENTS

The authors are grateful for a Marsden research grant and a Whitinga postdoctoral fellowship.

APPENDIX: INFINITE CYLINDER

The cylinder is another geometry where all surface points are identical, and total internal reflection is not excitable from rays outside. However, we cannot easily treat polarization, because the polarization of a ray relative to the cylinder surface changes between reflections. Nevertheless, we can get a reasonable approximation to the PLD by simply averaging the polarizations. This model is nonphysical for light, but a similar mathematical analysis will apply to (high-frequency) longitudinal waves, with a change of physical constants and reflectivity.

We imagine a scenario where the reflectivity is taken as the average of the two polarizations: $R = [R_s + R_p]/2$.

The chord length in a cylinder depends on θ_2 and also ϕ , the ray's rotation around the normal to the surface, where $\phi = 0$ points up the cylinder [2]:

$$C = \frac{2a \cos \theta_2}{1 - \sin^2 \theta_2 \cos^2 \phi}. \quad (A1)$$

This behaves similar to that in a slab when $\phi \approx 0$ or π , and similar to a sphere when $\phi \approx \pm\pi/2$. The PLD may be deduced from the integral for the mean path length over θ_2 , ϕ , substituting θ_2 , ϕ for θ_2 , C so that one can identify the integrand of the integral over C as the chord-length distribution. We leave the reflection and transmission as functions of θ_2

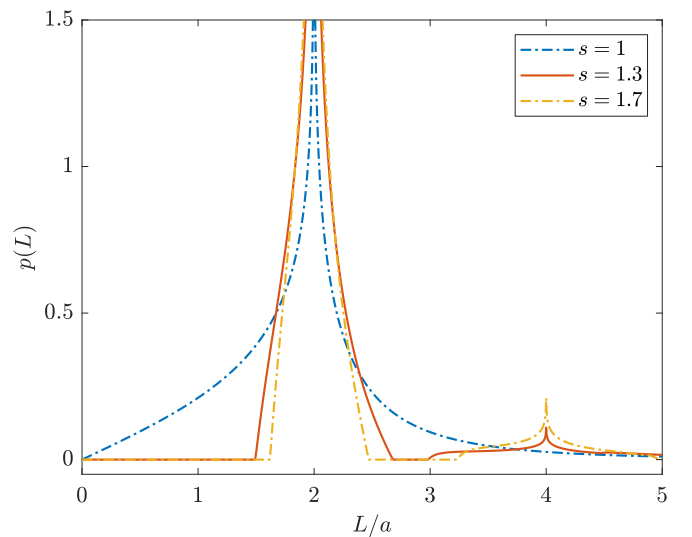


FIG. 6. Path-length distribution (A2) for an infinite cylinder of radius a , with averaged polarization effects. $p(L)$ diverges at $L/a = 2, 4, 6, \dots$ for $s > 1$.

to be integrated, $R(\theta_2)$, $T(\theta_2)$, and add the contributions from different numbers n of internal reflections. The result is

$$p(L) = R_F \delta(L) + \sum_{n=1}^{\infty} \int_{\theta_i}^{\theta_c} \frac{R(\theta_2)^{n-1}}{n} T(\theta_2)^2 \frac{4a}{\pi C} \times \frac{(\cos \theta_2)^{3/2} \sin \theta_2 d\theta_2}{\sqrt{(C - 2a \cos \theta_2)(2a - C \cos \theta_2)}} \Theta \left(2a \cos \theta_c \leq C \leq \frac{2a}{\cos \theta_c} \right), \quad (\text{A2})$$

where again $C = L/n$ and the lower integral bound is piecewise

$$\theta_i = \begin{cases} \cos^{-1} \frac{C}{2a} & C < 2a \\ \cos^{-1} \frac{2a}{C} & C \geq 2a. \end{cases} \quad (\text{A3})$$

This PLD is integrated numerically and plotted in Fig. 6. It agrees with Monte Carlo simulations (with averaged polarization effects) to within an error of 10^{-3} to 10^{-2} , and agrees with simulations that properly include polarization to within roughly a few percent.

-
- [1] R. Savo, R. Pierrat, U. Najar, R. Carminati, S. Rotter, and S. Gigan, Observation of mean path length invariance in light-scattering media, *Science* **358**, 765 (2017).
- [2] M. Majic, W. R. C. Somerville, and E. C. Le Ru, Mean path length inside nonscattering refractive objects, *Phys. Rev. A* **103**, L031502 (2021).
- [3] F. Martelli, F. Tommasi, L. Fini, L. Cortese, A. Sassaroli, and S. Cavaliere, Invariance properties of exact solutions of the radiative transfer equation, *J. Quant. Spectrosc. Radiat. Transfer* **276**, 107887 (2021).
- [4] M. Majic and W. R. C. Somerville, Mean path length in refractive regular polygons and prisms, *Phys. Rev. A* **105**, 023518 (2022).
- [5] M. Majic, W. Somerville, and E. C. Le Ru, Exploiting billiard theory to calculate the mean path length of light in refractive spheroids, *Phys. Rev. A* **106**, 013521 (2022).
- [6] W. Gille, Geometric figures with the same chord-length probability density function: Six examples, *Powder Technol.* **192**, 85 (2009).
- [7] Y. Grynko and Y. G. Shkuratov, Light scattering from particulate surfaces in geometrical optics approximation, in *Light Scattering Reviews 3* (Springer, New York, 2008), pp. 329–382.
- [8] O. Scheibelhofer, P. R. Wahl, B. Larchevêque, F. Chauchard, and J. G. Khinast, Spatially resolved spectral powder analysis: Experiments and modeling, *Appl. Spectrosc.* **72**, 521 (2018).
- [9] J. C. M. Anton, A. G. Manzanares, A. A. Fernandez-Balbuena, and D. V. Molini, Measuring the absorption coefficient of optical materials with arbitrary shape or distribution within an integrating sphere, *Opt. Express* **29**, 26287 (2021).
- [10] I. Sychugov, Analytical description of a luminescent solar concentrator, *Optica* **6**, 1046 (2019).
- [11] A. Malinka, E. Zege, G. Heygster, and L. Istomina, Reflective properties of white sea ice and snow, *Cryosphere* **10**, 2541 (2016).
- [12] R. Mupparapu, K. Vynck, T. Svensson, M. Burreli, and D. S. Wiersma, Path length enhancement in disordered media for increased absorption, *Opt. Express* **23**, A1472 (2015).
- [13] J. D. Jackson, *Classical Electrodynamics*, 3rd ed. (Wiley, New York, 1999).
- [14] S. Q. Duntley, The optical properties of diffusing materials, *J. Opt. Soc. Am.* **32**, 61 (1942).
- [15] E. Yablonovitch, Statistical ray optics, *J. Opt. Soc. Am.* **72**, 899 (1982).
- [16] H. M. Nussenzweig and W. J. Wiscombe, Efficiency Factors in Mie Scattering, *Phys. Rev. Lett.* **45**, 1490 (1980).
- [17] A. Kokhanovsky and E. Zege, Optical properties of aerosol particles: A review of approximate analytical solutions, *J. Aerosol Sci.* **28**, 1 (1997).
- [18] C. F. Bohren and D. R. Huffman, *Absorption and Scattering of Light by Small Particles* (Wiley, New York, 2008).
- [19] F. Tommasi, L. Fini, F. Martelli, and S. Cavaliere, Invariance property in scattering media and absorption, *Opt. Commun.* **458**, 124786 (2020).